Compositional and structural characterization of temperature-induced solid-state reactions in Al/Ni multilayers

U. Rothhaar, H. Oechsner, M. Scheib, and R. Müller
Fachbereich Physik und Institut für Oberflächen–und Schichtanalytik IFOS, Universität Kaiserslautern, D-67653 Kaiserslautern, Germany
(Received 19 August 1999)

Diffusion controlled solid-state reactions during the annealing of Al/Ni multilayers deposited by rf magnetron sputtering onto silicon substrates have been studied. The samples with an overall atomic concentration of $Al_{0.5}Ni_{0.5}$ consisted of four Ni and four Al sublayers with a double layer thickness of 50.3 nm. The temperature induced compositional and structural changes during the annealing periods of 45 min were determined by Auger electron spectroscopy (AES) sputter depth profiling and x-ray diffraction. Up to 120 °C no intermetallic phase was detected, albeit the AES sputter depth profiles indicated a significant enrichment of Ni in the Al layers. At temperatures around 160 °C these sublayers nucleated completely into the Al_3Ni phase. With a further increase of the annealing temperature the reaction proceeded to the formation of Al_3Ni_2, and finally above 250 °C to a homogeneous layer of bcc ordered AlNi.

I. INTRODUCTION

Intermetallic compounds formed by solid-state reactions in thin-film structures play an important role in heat and corrosion resistant coatings or in metallization layers of microelectronic devices, and have been the subject of considerable research.[1,2] Even when the pertinent thermodynamic information is available, the understanding and control of phase sequencing and of the respective solid-state reactions is rather difficult, and requires knowledge of the particle transport and the nucleation kinetics. Multilayer samples are highly suited to investigate the related interdiffusion mechanism and phase evolution, because they provide quite a number of reacting interfaces and well defined regions for the formation of intermetallic phases.

As an example of also technical importance,[3,4] the formation of aluminide films by temperature treatment of Al/Ni multilayers with an average composition of $Al_{0.5}Ni_{0.5}$ was studied in the present work. Previous investigations have shown in essence that Al_3Ni forms as the first crystalline phase in Al/Ni diffusion couples.[5–9] However, there is, for example, not yet clear evidence of the dominantly moving species in the initial stages of its growth. The Al/Ni system has been chosen since the corresponding phase diagram exhibits a limited number (five) of stable intermetallic compounds.[10] For the characterization of the temperature induced compositional and structural changes Auger electron spectroscopy (AES) sputter depth profiling and x-ray diffraction (XRD) were employed.

II. EXPERIMENT

The Al/Ni multilayers were prepared on smooth (100)-silicon substrates by rf-magnetron sputtering. The deposition chamber is a part of a complex ultrahigh vacuum (UHV) system which has been already described elsewhere,[11,12] and comprises separate chambers for sample introduction, surface analysis, and sample annealing. The individual Ni and Al sublayers were produced by two rf sputter magnetrons, which were equipped with high-purity Ni and Al targets and operated with Ar at 3.8×10^{-2} mbars (residual gas pressure 1×10^{-7} mbars). The substrates were alternately turned to the corresponding magnetron. The deposition time was controlled by a movable shutter in front of each sputter source.

In a first series of experiments pure Al and Ni films were deposited with a growth rate of about 20 Å/min for Ni and 40 Å/min for Al. These values were determined *ex situ* by thickness measurements with a mechanical step profilometer. With the particle densities $n(\mathrm{Ni})=9.13\times10^{22}\,\mathrm{cm}^{-3}$ and $n(\mathrm{Al})=6.02\times10^{22}\,\mathrm{cm}^{-3}$ taken from Ref. 13 a ratio $d(\mathrm{Al})/d(\mathrm{Ni})$ of 1.52 between the individual sublayer thicknesses d must be established to obtain an average 1:1 stoichiometry (50 at. % Al, 50 at. % Ni) in a multilayer stack. Based on these data the deposition times were chosen to produce samples consisting of four double layers, each of 20-nm Ni and 30.3-nm Al. Without breaking the vacuum the specimens were then directly transferred to the heating chamber and annealed by the radiation of halogen lamps at temperatures between 120 and 330 °C for always 45 min.

After cooling down to room temperature, the annealing induced compositional and structural changes were determined *ex situ* by AES sputter depth profiling and x-ray diffraction. The AES analyses were performed at a primary electron energy of 5 keV under bombardment with a raster-scanned 2-keV Ar^+ ion beam. An ion current density $j(Ar^+)$ of about 22 μA/cm^2 was used with exception of the sample annealed at 330 °C [$j(Ar^+)\approx43\,\mu$A/cm^2]. To convert the peak-to-peak amplitudes of the differentiated Al (KLL), Ni (LMM), Si (LMM), and O (KLL) Auger signals into concentrations, sensitivity factors were determined *in situ* for samples of well-known stoichiometry. With concern of the small total thickness of the multilayer structure of about 200 nm, the structural investigations were carried out with x-ray diffraction in a parallel beam geometry at an angle of x-ray incidence below 1° and the scattering plane perpendicular to the sample surface.

III. RESULTS

A. Unheated Al/Ni multilayer

The x-ray-diffraction pattern of the unheated sample in Fig. 1 contains only peaks of polycrystalline Al and Ni. It

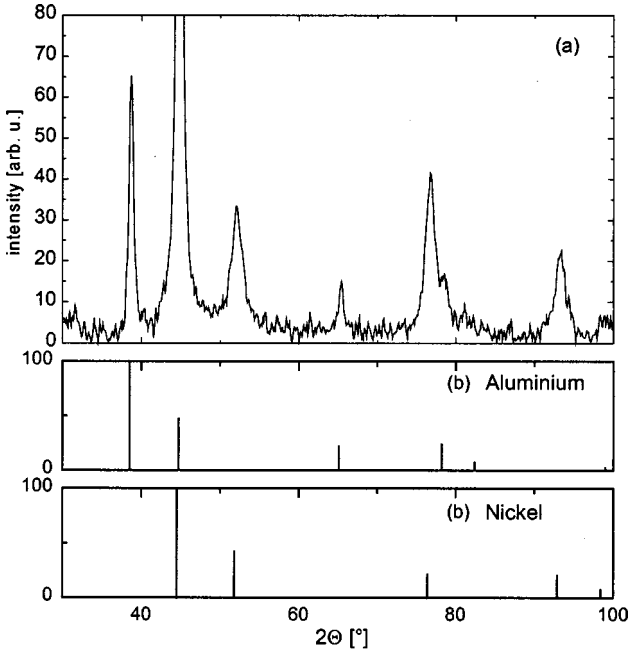

FIG. 1. Comparison of the XRD pattern of an as-deposited Al/Ni multilayer structure of a total thickness of 200 nm (a) with standard diffraction diagrams of Al and Ni (b).

should be noted that the enhancement of the Ni-diffraction peak at $2\theta = 76°$, referring to the (220) planes, indicates a (111) texture of the Ni sublayers in the sputter-deposited layer stacks. The corresponding AES concentration sputter time profile depicted in Fig. 2 displays the modulations of Al and Ni as expected for such an alternating structure. Because the time intervals for sputter removal of the individual Ni and Al sublayers are almost the same, and the total amount of particles is equal in each of them (average 1:1 composition), the differences of the elemental sputter yields Y of Al and Ni under 2-keV Ar^+ bombardment must be small. This finding compares well with previously reported Y(Al) and Y(Ni) values.[14]

An aspect—astonishing in the first instance—of Fig. 2 is the presence of Ni with about 13 at. % in the three ''hidden'' aluminum layers, contrary to the composition of the uppermost Al layer. A similar behavior was observed by others in AES sputter depth profiles of Al/Ni multilayers with a

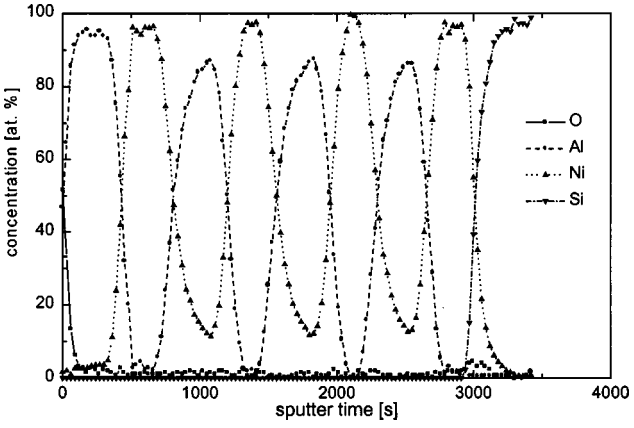

FIG. 2. Concentration vs sputter time profile of an as-deposited Al/Ni multilayer on Si substrate.

double layer thickness of 63 nm, and was ascribed to Ni diffusion during the film preparation.[15] This explanation seems unsuitable in the present case because the deposition temperature did not exceed 50 °C, and diffusion induced phenomena should for time reasons be more pronounced in the deeper lying Al sublayers being deposited at first. Additionally, the Al→Ni interfaces remain always sharper than that for Ni→Al.

Similarly, in depth profiles of Ta/Si multilayer structures measured with secondary neutral mass spectrometry (SNMS) Ta was found to move into the next deeper Si sublayer but not vice versa.[16] Hence the analyzing process itself is probably the reason for the measured Ni concentration profiles. A plausible explanation in both cases might be obtained from collisional (or radiation) enhanced particle transport across the interfaces and preferential sputter removal of the lighter constituent Al or Si when the mixed interface region is forming. This is in accordance with other studies, in which Al has been found to be preferentially sputter removed from the surface of Al-Ni alloys under keV ion bombardment.[17,18]

Additional depth profiling of an unheated layer stack with the mass spectrometric $M\mathrm{Cs}^+$-technique[19] (M stands for Ni or Al in the present case) employing 5.5-keV Cs^+ ions for sputter removal resulted not only in a reduction of the experimental width of the Ni→Al interfaces by a factor of about 2.5 compared to the AES-sputter profiles in Fig. 2. Moreover, the presumably fictitious Ni content in the Al layers was found to be only 3–4 at. %. Such differences can be understood from the shallower information depth of about 2–3 atomic layers with the $M\mathrm{Cs}^+$ technique compared to the mean escape depth of about 8 monolayers of the 848 eV Ni (LMM)-Auger electrons. Like the AES profile in Fig. 2 the $M\mathrm{Cs}^+$ profiles display a pronounced asymmetry of the interfaces: The Ni→Al—transitions are always followed by a Ni tail into the next deeper Al sublayer, whereas the Al→Ni interface is always steeper, and zero Al—concentration is rapidly reached in the next deeper Ni sublayer. It is this asymmetry in the sputter profiles which indicates the profiling ion bombardment to cause Ni to move into Al but not vice versa. Thus the depth profiles of the unheated layer stacks indicate already the Ni atoms to be the more mobile species in the Al-Ni system.

B. Annealed multilayers

1. *Temperature* $T = 120\,°\mathrm{C}$, *heating time* $t = 45$ min

The structural information from the XRD diagram of an Al/Ni multilayer annealed at 120 °C for 45 min differs not significantly from that of the as-deposited sample. Only the intensities of the Al peaks were reduced. On the other hand, the concentration sputter time profile (Fig. 3) derived from the AES signals shows an increased Ni content of more than 20 at. % in the Al layers, while there is still no indication of aluminum in the Ni films. Again the sputter induced interface effects are visible.

Although the reaction partners were now mixed to some extent, no ordered Al/Ni phase has grown. This indicates the formation of regions with an Al-rich solid solution where the Ni concentration exceeds the equilibrium solubility of 0.025 at. %.[10] Such supersaturated solid solutions in the Al/Ni system are known to occur during the rapid cooling of liquid

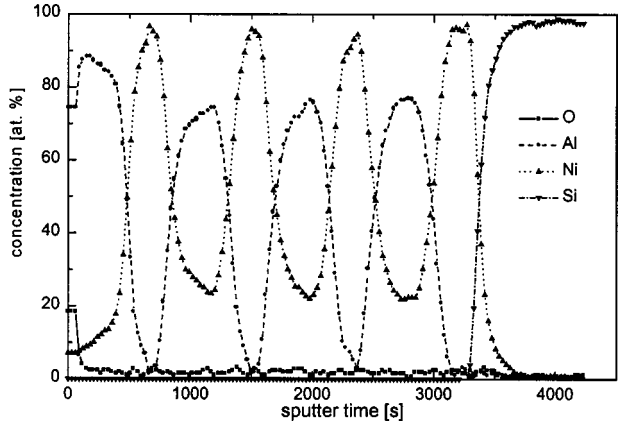

FIG. 3. Concentration vs sputter time profile of a sample after annealing at 120 °C for 45 min.

alloys (7.7 at. % Ni in Al),[20] or by quenching from the vapor phase (up to 20.9 at. % Ni in Al).[10] The observed mixing effect seems to be determined by a higher mobility of the Ni particles in Al. This is corroborated by the differences of the activation energy for the diffusion of Al in Ni [64 kcal/mol,[21] 62.1 kcal/mol (Ref. 22)] and of Ni in Al [35 kcal/mol (Ref. 23)]. Of course, additional factors such as a high defect density or residual stress can affect the diffusion behavior in thin-film structures. This may explain the deviating conclusions of different authors about the dominantly moving species during low-temperature interdiffusion in Al/Ni systems.[3–7] The higher mobility of Ni in Al may—besides ion bombardment effects—also contribute to the broadening of the Ni→Al interfaces observed in the AES sputter depth profiles. Both influences can, however, hardly be separated from each other.

2. $T = 160\,°C$, $t = 45$ min

An increase of the annealing temperature from 120 to 160 °C, i.e. of only 40 °C, leads to a pronounced structural transition within the multilayer. As can be seen from the XRD spectrum in Fig. 4(a) the diffraction peaks of elemental Al have disappeared, and adjacent to the main Ni peak, new peaks appear which are characteristic for the crystalline Al_3Ni phase (cf. to Fig. 4(b) with the ICDD standards[24] of Al_3Ni and Ni). The measured concentration-vs-erosion time profile in Fig. 5 displays a further increased Ni content (36 at. %) in the Al films which are still separated by pure Ni layers. Again the existence of a (110) texture in the still present Ni sublayers becomes visible from the increased Ni(220) x-ray-diffraction peak around 76° in Fig. 4(a).

According to the results in Figs. 4 and 5, Al_3Ni is the first intermetallic compound to form when the Al/Ni multilayer structure is annealed at a sufficiently high temperature. The growth of this phase is evidently determined by the diffusion of Ni into the Al layers. There is no experimental indication for the existence of a crystalline metastable compound (η phase, Al_9Ni_2) as observed in other studies when annealing Al/Ni multilayers of considerably larger single layer thicknesses between 80 and 400 nm.[4] Because there exists no solid solution of Ni in Al with a concentration close to the Al_3Ni stoichiometry,[8] and there are no indications for another Al-Ni phase, the whole Al of the layer structure with

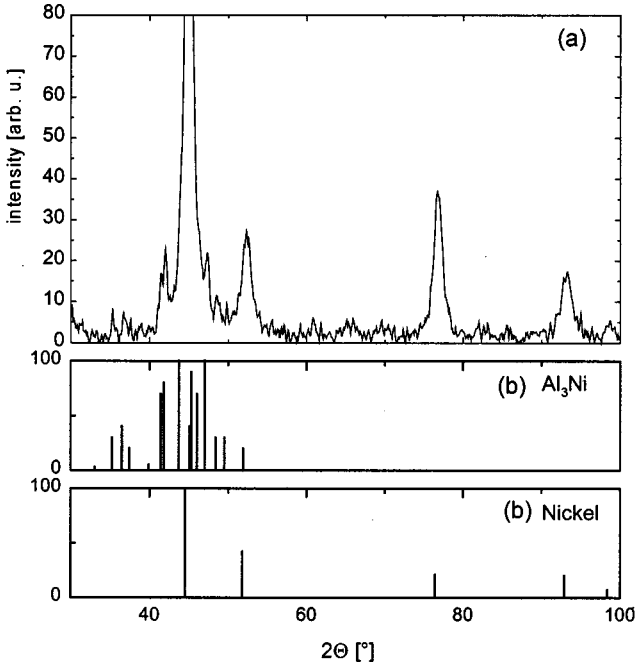

FIG. 4. Comparison of the XRD spectrum of an Al/Ni multilayer after annealing at 160 °C for 45 min (a) with standard diffraction diagrams of Al_3Ni and Ni (b).

the exception of some parts of the topmost Al layer reacted into the Al_3Ni configuration. The Al_3Ni sublayers in the now generated Al_3Ni/Ni multilayer structure should contain 25 at. % Ni. The higher Ni concentrations in Fig. 5 as derived from the AES signals can readily be ascribed to the already mentioned ion bombardment effects. The increase of the Ni concentration by about 10% over the nominal value for Al_3Ni fits well with the results from the unbaked sample. Thus the small plateau in the topmost Al layer confirms also the formation of Al_3Ni by an atomic transport from the underlying Ni layer.

3. $T = 200\,°C$, $t = 45$ min

After heat treatment at 200 °C for 45 min advanced structural changes were observed. The corresponding x-ray diffraction pattern (Fig. 6) clearly provides evidence for the formation of the Al_3Ni_2 phase, whereas any more peaks cor-

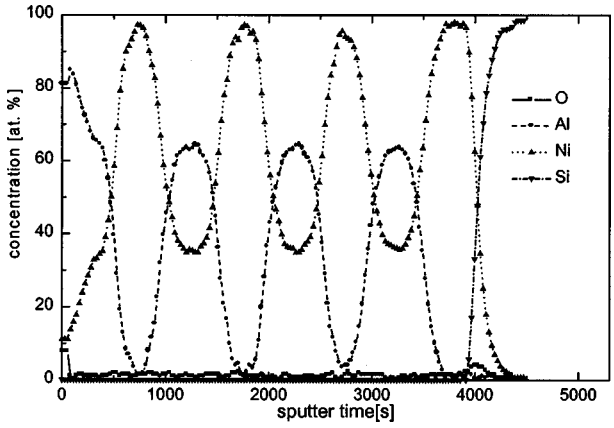

FIG. 5. Concentration vs sputter time profile of an Al/Ni multilayer sample annealed at 160 °C for 45 min.

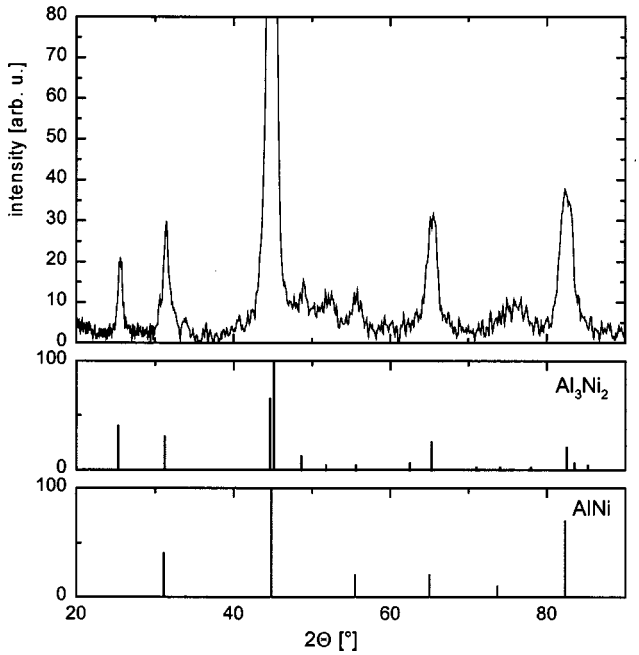

FIG. 6. X-ray-diffraction pattern for an Al/Ni multilayer annealed at 200 °C (a) compared with the standards of Al_3Ni_2 and AlNi (b).

responding to Al_3Ni are detectable. Especially the diffraction peaks at 25.5° and 48.6° are attributed to the (100) and (111) planes of the Al_3Ni_2 phase. Additionally, the reacted layers may already include small amounts of AlNi. A separation of the AlNi—from the Al_3Ni_2—peaks was not possible because of the not sufficiently high angular resolution of the XRD equipment. The corresponding AES depth profiles (not shown here) reveal that the modulations of the Al and Ni concentrations are now strongly reduced. Since about 35 at. % Al is found in the initial Ni layers, the AES profile indicates now that both Ni and Al had moved.

4. $T = 330\,°C$, $t = 45$ min

With a further increase of the annealing temperature the shape of the AES sputter profiles approaches continuously that in Fig. 7 (330 °C, 45 min). The original alternating Al/Ni

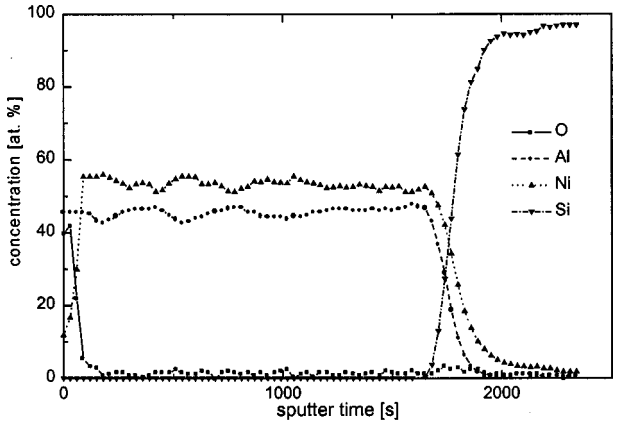

FIG. 7. Concentration vs sputter time profile of an Al/Ni multilayer after annealing at 330 °C for 45 min.

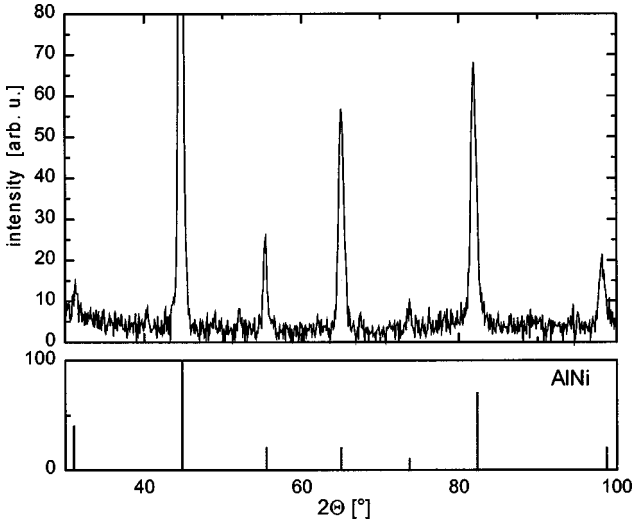

FIG. 8. XRD spectrum of an Al/Ni multilayer sample annealed for 45 min at 330 °C.

structure has disappeared, and with the exception of the partly oxidized surface region one layer with almost homogeneous Al and Ni concentrations has evolved. Hence the entire multilayer has reacted during the heating procedure. The longer tail of the Ni profile in the Si substrate (compared to that of Al) can be ascribed to the differences of the respective diffusion coefficients. While the mobility of Al in Si is negligible at temperatures around 300 °C,[25] the Ni-Si system already starts to form silicides.[26] The x-ray spectrum of a sample annealed at 330 °C is depicted in Fig. 8 and shows only peaks corresponding to AlNi as a representative of the group of bcc-structured Hume Rothery phases. An average grain size of 45 nm is obtained from the width of the diffraction lines, which exceeds the thickness of the initial single layers.

IV. DISCUSSION

While several conclusions about the mechanism of the investigated temperature induced solid-state reactions have already been drawn in the previous section, some synoptic features will be discussed now. In Fig. 9 the Ni content in the

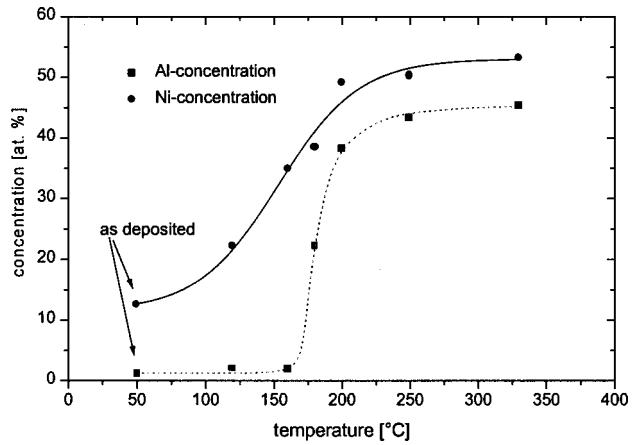

FIG. 9. Al and Ni concentration in the center of the initially pure Ni and Al sublayers, respectively.

''Al'' layers and the Al content in the ''Ni'' layers is depicted as a function of the heating temperature (the annealing time was always 45 min). The respective values were always taken from the center of the corresponding sublayers as being displayed by the AES concentration sputter time profiles. As already mentioned in Sec. III B 1, the initial stages of the solid-state reaction in the investigated Al/Ni system were up to 160 °C exclusively controlled by the diffusion of Ni into the Al sublayers. The steplike increase of the Al concentration in the ''Ni films'' at 160 °C indicates the onset of an additional contribution from moving Al atoms to the particle transport as the mandatory condition for the solid-state reaction towards AlNi. As can be seen from Fig. 9, a further increase of the annealing temperature leads to an almost homogeneous film after heat treatment above 250 °C. The slightly lower values of the Al concentrations derived from the AES signals must again be referred to the preferential sputtering effect for Al from an AlNi surface.

The different Al-Ni phases formed by the annealing procedure at different temperatures are summarized in Table I. The initial formation of Al_3Ni confirms Bené's[27] rule for the interfacial reaction between two thin metallic films at moderate temperatures. This rule predicts that the first phase nucleating in such structures is neighbored to the low-temperature eutectic in the binary phase diagram, i.e., to Al in our system. Hence Al_3Ni as the Al richest phase should form at first. Thermodynamic considerations on the basis of the differences of the free energy ΔG (Refs. 6 and 8) favor always the formation of AlNi in the present case. Therefore the thermodynamic driving forces derived from equilibrium diagrams are not suitable to explain the observed phase sequencing. This is not surprising, because thermal equilibrium conditions were intentionally not achieved in our experiments. When considering the combined information of the structural (XRD) and the depth resolved compositional changes (AES), we conclude that the particle transport rather than the obviously much faster nucleation step dominates the solid-state reaction of the system Al-Ni. Especially the nucleation into Al_3Ni, which was preceded by the formation of an Al-rich solid solution, is controlled by the supply of Ni into the Al regions.

This result compares with previous findings where the growth of Al_3Ni in Al/Ni thin-film systems is found to be diffusion limited with a parabolic time (t) behavior.[3,28] Therefore the relation $d^2 = Kt$ should be valid for the thickening d of the Al_3Ni phase (K = reaction-rate constant). In the present case, the entire Al was found to react into Al_3Ni after a heat treatment at 160 °C for 45 min (Figs. 4 and 5). Hence for the respective reaction-rate constant K a lower limit of $1.17\times10^{-15}\,\mathrm{cm^2/s}$ can be readily calculated under neglection of possible grain-boundary processes. From the relation $K = 0.387\cdot\exp(-1.4\,\mathrm{eV/kT})\,\mathrm{cm^2/s}$ which was derived for the formation of Al_3Ni on large-grain aluminum crystals,[28] a reaction-rate constant of only $2\times10^{-17}\,\mathrm{cm^2/s}$ is calculated for 160 °C. The difference of both K values is most probably due to the microcrystalline film structure in our experiments, which provides in comparison with the conditions in Ref. 28 an enlarged reaction front across the grain boundaries in addition to that at the film interfaces. Compared to such effects, the influence of a certain texture of the Ni sublayers (see Figs. 1 and 4) serving as the sources of the migrating Ni atoms might, however, be of less importance.

TABLE I. Solid-state Al-Ni phases forming by annealing at different temperatures for 45 min ●: clearly proved, (●): small contributions possible.

	Observed phases				
Temperature	Al	Ni	Al_3Ni	Al_3Ni_2	AlNi
As deposited (≤ 50 °C)	●	●			
120 °C	●	●			
160 °C		●	●		
180 °C		●	●	(●)	(●)
200 °C		(●)		●	(●)
250 °C				●	●
330 °C					●

V. CONCLUSIONS

The solid-state reactions in Al/Ni multilayers with an average composition of 1:1, which were prepared and annealed *in situ* under ultrahigh vacuum conditions, have been investigated. The combination of compositional (AES sputter depth profiling) and structural (XRD) analyses was shown to deliver detailed information about the sequence of intermediate alloys which are formed along the reaction path from elemental Ni and Al towards the final NiAl phase. With increasing annealing temperature a metastable solid solution of Ni in Al is formed at first with Ni as the dominantly moving species. Subsequently, Al_3Ni as the first intermetallic phase nucleates in the previously interdiffused regions under annealing at 160 °C. At increased temperatures the reaction proceeds to Al_3Ni_2 as the next Ni richer intermetallic compound in the Al-Ni system. Finally, after a heat treatment above 250 °C the concentration modulations in the Al/Ni-multilayer system vanished almost completely, and according to its average composition the entire layer stack was converted into AlNi as an example for a bcc-ordered Hume Rothery phase.

ACKNOWLEDGMENTS

The present work is part of a project in the Schwerpunktsprogramm ''Reaktivität von Festkörpern'' of the Deutsche Forschungsgemeinschaft. Financial support from this organization is gratefully acknowledged. Thanks are due to H. Gnaser (IFOS Kaiserslautern) for the MCs^+-depth profiling measurements.

[1] P. Hannu, P. Kattelus, and M. A. Nicolet, in *Diffusion Phenomena in Thin Films and Microelectronic Materials*, edited by D. Gupta and P. S. Ho (Noyes Publications, Park Ridge, NJ, 1988), p. 432.
[2] F. Fitzer and J. Schlichting, in *High Temperature Corrosion*, edited by R. A. Rapp (National Association of Corrosion Engineers, Houston, TX, 1983), p. 604.
[3] D. B. Miracle, Acta Metall. Mater. **41**, 649 (1993).
[4] R. Darolia, D. F. Lahrman, R. D. Field, J. R. Dobbs, K. M. Chang, E. H. Goldman, and D. G. Konitzer, in *Ordered Intermetallics-Physical Metallurgy and Mechanical Behavior*, edited by C. T. Liu, R. W. Cahn, and G. Sauthoff (Kluwer Academic, Dordrecht, 1992), p. 679.
[5] E. Ma, C. V. Thompson, and L. A. Clevenger, J. Appl. Phys. **69**, 2211 (1991).
[6] A. S. Edelstein, R. K. Everett, G. Y. Richardson, S. B. Qadri, E. I. Altman, J. C. Foley, and J. H. Perepezko, J. Appl. Phys. **76**, 7850 (1994).
[7] A. Zalar, S. Hofmann, F. Pimentel, D. Kohl, and P. Panjan, Vacuum **46**, 1077 (1995).
[8] E. G. Colgan, M. Nastasi, and J. W. Mayer, J. Appl. Phys. **58**, 4125 (1985).
[9] R. J. Torento and G. Blaise, Acta Metall. **37**, 2305 (1989).
[10] B. Predel, in *Phase Equilibria, Crystallographic and Thermodynamic Data of Binary Alloys*, edited by O. Madelung, Landolt-Börnstein, New Series, Group IV, Vol. 5a (Springer, Berlin, 1991), p. 212.
[11] U. Rothhaar and H. Oechsner, Surf. Coat. Technol. **59**, 183 (1993).
[12] V. Rupertus, U. Rothhaar, P. Köpfer, A. Lorenz, and H. Oechsner, Vak. Prax. **5**, 183 (1993).
[13] *Handbook of Chemistry and Physics*, edited by R. C. Weast (CRC Press, Boca Raton, FL, 1986).
[14] *Sputtering by Particle Bombardment*, edited by R. Behrisch (Springer, Berlin, 1981), Vol. I.
[15] A. Zalar, S. Hofmann, D. Kohl, and P. Panjan, Thin Solid Films **270**, 341 (1995).
[16] A. Wucher and H. Oechsner, Fresenius Z. Anal. Chem. **333**, 470 (1989).
[17] M. P. Thomas and B. Ralph, Surf. Sci. **124**, 129 (1983).
[18] M. P. Thomas and B. Ralph, Surf. Sci. **124**, 151 (1983).
[19] H. Gnaser and H. Oechsner, Fresenius J. Anal. Chem. **341**, 54 (1991).
[20] A. Tonejc, D. Rocák, and A. Bonefacic, Acta Metall. **19**, 311 (1971).
[21] K. Hauffe, *Reaktionen in and an festen Körpern* (Springer, Berlin, 1966).
[22] W. Gust, M. B. Hintz, A. Lodding, H. Odelius, and B. Predel, Phys. Status Solidi A **64**, 187 (1981).
[23] *Smithells Metals Reference Book*, 6th ed., edited by C. J. Smithells (Butterworths, London, 1983).
[24] International Center for Diffraction Data, Swarthmore, PA, Powder Diffraction File 1989.
[25] R. N. Ghoshtagore, Phys. Rev. B **3**, 2507 (1971).
[26] G. L. P. Berning and L. L. Levenson, Thin Solid Films **55**, 473 (1978).
[27] R. W. Bené, Appl. Phys. Lett. **41**, 529 (1982).
[28] X.-A. Zhao, M.-Y. Yang, E. Ma, and M.-A. Nicolet, J. Appl. Phys. **62**, 1821 (1987).